Remodelling a shp: Transmetallation in a Rare-Earth Cluster-based Metal–Organic Framework

Hudson A. Bicalho[ab], P. Rafael Donnarumma[ab], Victor Quezada-Novoa[ab], Hatem M. Titi[c], Ashlee J. Howarth[ab*]

[a] *Department of Chemistry and Biochemistry, Concordia University, 7141 Sherbrooke St W., Montréal, QC, Canada*
[b] *Centre for NanoScience Research, Concordia University, Montréal, QC, Canada*
[c] *Department of Chemistry, McGill University, 801 Sherbrooke St W., Montréal, QC, Canada*

ABSTRACT: Post-synthetic modification (PSM) of metal–organic frameworks (MOFs) is an important strategy for accessing MOF analogues that cannot be easily synthesized *de novo*. In this work, the rare-earth (RE) cluster-based MOF, Y-CU-10, with **shp** topology was modified through transmetallation using a series of RE ions, including: La(III), Nd(III), Eu(III), Tb(III), Er(III), Tm(III), and Yb(III). In all cases, metal-exchange higher than 70 % was observed, with reproducible results. All transmetallated materials were fully characterized and compared to the parent MOF, Y-CU-10, in regards to crystallinity, surface area, and morphology. Additionally, single-crystal X-ray diffraction (SCXRD) measurements were performed to provide further evidence of transmetallation occurring in the nonanuclear cluster nodes of the MOF.

1. Introduction

Metal–organic frameworks (MOFs) are a family of structurally diverse and porous materials comprised of concatenated organic building blocks, known as linkers, and inorganic building units extending in 2- or 3-dimensions.[1–6] The rapid development of MOFs in the past few decades has spawned a myriad of materials with varied architectures and functionalities.[7] Due to their chemical and physical properties, MOFs have potential applications in several fields including, but not limited to, catalysis,[8–11] gas adsorption and storage,[12–14] chemical sensing,[15,16] and light harvesting.[17]

MOFs can be designed *de novo* through the use of reticular chemistry.[18] After selecting the appropriate metal nodes and organic linkers to give a desired topology, synthetic conditions must then be controlled to facilitate metal-ligand bonding with suitable geometry and connectivity. Nonetheless, it can be challenging to control reaction conditions to obtain a desired topology, since many metal and organic precursor combinations can give rise to multiple possible topologies.[19] One way to circumvent this challenge and to avoid rigorous synthetic optimization, is through the use of post-synthetic modification (PSM) strategies.[20] PSM is a group of methodologies that involves the modification of parent MOFs into novel daughter frameworks exhibiting different, and sometimes enhanced, properties compared to their predecessors.[21,22] There are several different types of PSM methods, which include modifying the MOF linker, node, or encapsulating guests inside the framework. Linker-based PSM in MOFs includes (i) linker modification (i.e., covalent PSM), where the linker in the structure is chemically modified while still part of the MOF,[23,24] (ii) linker exchange (i.e., solvent assisted linker exchange (SALE),[25] or post-synthetic exchange (PSE)[26]), in which a linker is exchanged for a different one, or (iii) post-synthetic annealing (PSA), where linkers and capping ligands in a MOF are rearranged.[27] On the other hand, metal-based PSM of MOFs includes (i) transmetallation, where the metal is replaced with a new metal that can adopt the same coordination number and geometry,[28,29] (ii) atomic layer deposition in a MOF (AIM) where metal ions/clusters are deposited on a MOF metal node,[30,31] or (iii) solvent assisted metal insertion (SAMI), where metal ions are post-synthetically coordinated to a MOF metal node.[32,33] Transmetallation, in particular, is one strategy that can be used to access MOF analogues that are difficult to synthesize *de novo*. The partial or complete substitution of a metal in a MOF, through transmetallation, has the potential to lead to a daughter material with new properties such as enhanced catalytic activity or adsorption. In general, the degree of transmetallation in a MOF will be governed by a series of factors, including the lability of the M-L bond, the ionic radii of the incoming *vs.* outgoing metal ion, the preferred coordination number and geometries of the incoming and outgoing metal ion, the solvent used, and the chemical stability of the parent and daughter MOFs.[34]

Rare-earth (RE) elements, which include Y, Sc and the 15 *f*-block lanthanoids, are a group of metals that share similar chemistry and are therefore expected to behave similarly in regards to MOF synthesis and structure.[35] However, *de novo* synthesis of isostructural RE-MOFs comprised of each of the 17 RE elements can be challenging due to the variability in

ionic radii and preferred coordination number of these ions.[36] *De novo* synthesis can be particularly challenging when constructing RE-MOFs with high nuclearity cluster-based nodes, since the lability and thus stability of the RE-clusters vary with ionic radii. For this reason, PSM, specifically transmetallation, is attractive for the synthesis of new RE-MOFs not easily attainable *de novo*. In that sense, transmetallation is an effective way of incorporating or completely substituting new RE ions into a parent MOF, be it *via* metal (non-RE) to RE ion,[37–39] or RE to RE ion exchange.[40–42] However, to this date, only a few examples of transmetallation in RE-MOFs have been shown in the literature,[40–42] and to the best of our knowledge, none involve RE-cluster based MOFs.

Herein, we report the transmetallation of Y(III) ions for other RE(III) ions (RE(III) = La(III), Nd(III), Eu(III), Tb(III), Er(III), Tm(III), and Yb(III)) in Y-CU-10. This MOF is comprised of nonanuclear cluster nodes bridged by tetratopic pyrene-based linkers, giving rise to a framework with **shp** topology (Figure 1). Attempts to synthesize RE-CU-10 analogues (RE(III) = La(III), Nd(III), Eu(III), Tb(III), Er(III), Tm(III), and Yb(III)) *de novo* through the direct translation of synthetic conditions for Y-CU-10 (i.e., simply using the same molar ratio of metal ion precursor) have been unsuccessful. Indeed, a recent report on the synthesis of Eu-CU-10/PCN-502(Eu) demonstrates that synthetic conditions are quite different than those used for Y-CU-10.[43] As such, the results shine light on transmetallation as a viable approach for obtaining difficult-to-synthesize RE-MOF analogues. The daughter MOFs are fully characterized, demonstrating a high degree of transmetallation, while maintaining the expected network structure. Furthermore, single crystal X-ray diffraction (SCXRD) of the transmetallated Tm-CU-10 analogue demonstrates that the incoming Tm(III) ion is incorporated into the nonanuclear cluster node of the MOF.

2. Experimental Section

2.1 Materials

All chemicals were used as received. *N,N'*-dimethylformamide (DMF), acetone, methanol, nitric acid, hydrogen peroxide (30 %, w/w) and glacial acetic acid (HAc) were purchased from Fisher Scientific. 2-fluorobenzoic acid, yttrium(III) nitrate hexahydrate [Y(NO$_3$)$_3$.6H$_2$O], lanthanum(III) nitrate hexahydrate [La(NO$_3$)$_3$.6H$_2$O], neodymium(III) nitrate hydrate [Nd(NO$_3$)$_3$.xH$_2$O], europium(III) nitrate hexahydrate [Eu(NO$_3$)$_3$.6H$_2$O], terbium(III) nitrate hydrate [Tb(NO$_3$)$_3$.xH$_2$O], erbium(III) nitrate hydrate [Er(NO$_3$)$_3$.xH$_2$O], thulium(III) nitrate hydrate [Tm(NO$_3$)$_3$.xH$_2$O], and ytterbium nitrate hydrate [Yb(NO$_3$)$_3$.xH$_2$O] were purchased from Alfa Aesar.

2.2. Synthesis of Y-CU-10

The 4,4',4'',4'''-(pyrene-1,3,6,8-tetrayl)tetrabenzoic acid (H$_4$TBAPy) linker was synthesized following a reported procedure.[44] In a typical synthesis of Y-CU-10,[45] Y(NO$_3$)$_3$.6H$_2$O (249.3 mg, 0.652 mmol), H$_4$TBAPy (111.0 mg, 0.163 mmol), and 2-fluorobenzoic acid (4560.6 mg, 32.5 mmol) were mixed with 28.3 mL of DMF, 2.3 mL (130 mmol) of deionized water and 6.1 mL (106 mmol) of HAc.
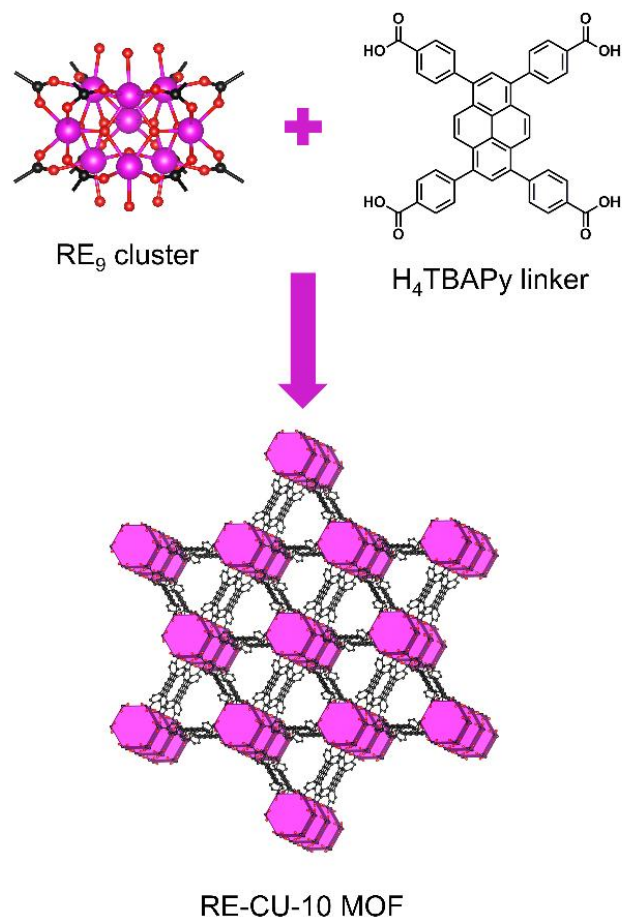

Figure. 1. Structure of RE-CU-10, showing the nonanuclear RE-cluster node and H$_4$TBAPy linker.

This suspension was homogenized by sonication for 10 minutes and then equally transferred to three 8-dram vials, which were placed in a preheated oven at 120 ºC for 48 h. The obtained yellow crystals were separated *via* centrifugation and washed three times with fresh DMF over the course of 24 h. Solvent exchange was conducted by replacing DMF and washing the MOF three times with fresh acetone over the course of 24 h. Finally, the material was air dried and activated at 120 ºC for 12 h under vacuum.

2.3 Transmetallation of Y-CU-10

In the optimized transmetallation procedure, 2.75 mmol of Y-CU-10 (10 mg, 24.76 mmol of Y) was added to 5 mL of a DMF solution containing 5 eqv. (123.8 mmol) of the RE(NO$_3$)$_3$.xH$_2$O salt (RE = La, Nd, Eu, Tb, Er, Tm, Yb). The reaction mixture was then placed in a preheated oven at 140 ºC for 14 days. After 3, 7 and 11 days, the material was collected and washed three times with fresh DMF, and the RE(NO$_3$)$_3$.xH$_2$O salt solution was replaced by a new one (123.8 mmol in 5 mL of DMF). The obtained materials were washed three times with DMF over the course of 24 hours, followed by washing with fresh acetone over the course of 24 hours. The materials were air dried and activated at 120 ºC for 12 h under vacuum. The degree of transmetallation was measured by inductively coupled plasma mass spectrometry (ICP-MS). For comparison purposes, all

transmetallation reactions were performed in quadruplicates.

2.4 Characterization

Powder X-ray diffraction patterns were recorded using a Bruker D2 Phaser diffractometer with Cu$K\alpha$ irradiation (λ = 1.54178 Å) equipped with a LYNXEYE linear position sensitive detector (Bruker AXS, Madison, WI) over a range of 4° < 2θ < 20° at a scan rate of 6° min^{-1}. Brunauer-Emmett-Teller (BET) specific surface area measurements were determined by N_2 adsorption-desorption isotherms collected at 77 K on a Micromeritics TriStar II Plus instrument. Prior to the analysis, the samples were subject to washing and solvent exchange with DMF followed by acetone, and then activated at 120 ºC for 12 h using a Micromeritics Smart VacPrep instrument equipped with a hybrid turbo vacuum pump. Scanning electron microscopy (SEM) images and energy-dispersive X-ray (EDX) spectroscopy were recorded on a Phenom ProX Desktop SEM instrument. ICP-MS measurements were carried out using a 7500 Agilent 7500ce equipment. Prior to the analysis, 0.5–1.0 mg of MOF sample was added to 0.8 mL of concentrated HNO_3 and heated at 100 ºC for 1 h in a sand bath. Then, after cooling down to room temperature, 0.2 mL of H_2O_2 (30%, w/w) was added to the mixture and heated at 100 ºC for another 2 h. Finally, the samples were sonicated for 30 minutes or until complete solubilization. The volumes of the digested samples were first adjusted to 10 mL using MilliQ water, and then further diluted 30 times. Crystals of transmetallated Tm-CU-10 were coated with a thin layer of amorphous oil and mounted on single crystal X-ray diffraction (SCXRD) at room temperature. Data were measured on a Bruker D8 Venture diffractometer equipped with a Photon 200 area detector, and $I\mu S$ microfocus X-ray source (Bruker AXS, Cu$K\alpha$ source).

3. Results and Discussion

Y-CU-10 is one of a handful of RE-MOFs found in the literature comprised of a highly connected, high nuclearity (> 6 ions) cluster node.[46–49] Owing to the high chemical and thermal stability of Y-CU-10, as well as the 12 Å channels, our group recently demonstrated that Y-CU-10 is a highly effective catalyst for the oxidative detoxification of a sulfur mustard simulant *via* the production of singlet oxygen ($^1O_2$).[45] Furthermore, by substituting Y(III) for heavier rare-earth metals, such as Tb(III), enhanced catalytic activity is observed. However, the synthesis of RE-CU-10 analogues has been challenging, as the synthetic procedure cannot be directly translated from that developed for Y-CU-10, resulting in a series of issues related to phase impurities (Figure S1), and low yields. Thus, in an attempt to access additional RE analogues of Y-CU-10, we performed metal-exchange (i.e., transmetallation) of the Y(III) ions using other RE(III) precursors (RE(III) = La(III), Nd(III), Eu(III), Tb(III), Er(III), Tm(III), and Yb(III)), to yield a series of RE-CU-10 analogues, most of which could not be obtained *de novo*.

To determine if transmetallation could be performed on Y-CU-10, methanol and DMF were screened as reaction solvents at 60 and 120 ºC, respectively (Figure S2, Table S1). While metal-exchange in the presence of methanol has shown promising results in previous works,[50,51] DMF can
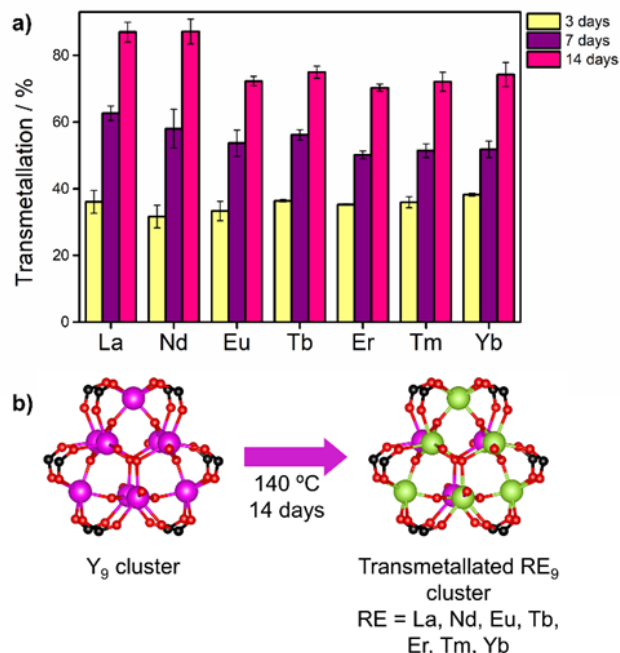

Figure 2. a) The degree of transmetallation in Y-CU-10 when using eight different RE(III) precursors and b) the nonanuclear cluster of CU-10 before and after the transmetallation experiments (pink spheres = Y(III); green spheres = RE(III)).

be heated at higher temperatures (boiling point: 64.7 *vs.* 153 ºC, respectively) and has also proven to be an effective solvent for transmetallation.[52,53]

After 7 days of reaction in methanol at 60 ºC using 5 equivalents of RE(III) precursor, approximately 5 % and 7 % of the Y(III) ions of Y-CU-10 were exchanged by Eu(III) or Tb(III), respectively. On the other hand, when DMF was used as a reaction solvent at 120 ºC using the same molar ratio of RE(III) ion precursor, exchange of 14 % (Eu) and 15 % (Tb) of the Y(III) ions in Y-CU-10 was observed after only 3 days of reaction. These preliminary results indicate that higher temperature enhances the transmetallation process in Y-CU-10. Additional attempts at optimizing the degree of transmetallation were carried out by increasing the reaction temperature in DMF from 120 to 140 ºC, as well as the amount of RE(III) precursor from 5 to 10 equivalents (Figure S3, Table S2). Not surprisingly, both increasing the RE(III) precursor concentration and increasing the temperature to 140 ºC were found to enhance the transmetallation efficiency in Y-CU-10. For example, after 7 days of reaction in DMF using 10 equivalents of RE(III) precursor, transmetallation of Tb(III) was enhanced from 22 to 60 % while that of Eu(III) was enhanced from 29 to 58 %, when changing the temperature from 120 to 140 ºC. Furthermore, by increasing the reaction time at 140 ºC in DMF to 14 days, and the amount of RE(III) precursor from 10 to 15 equivalents (Figure S4, Table S3), exchange as high as 91 % for Eu(III) was observed. These results demonstrate that near complete transmetallation of the Y(III) ions in Y-CU-10 with other RE(III) ions is possible.

Given that some RE(NO$_3$)$_3$·xH$_2$O precursors are expensive, and that even partial substitution of the Y(III) ions with RE(III) ions is expected to endow the daughter framework with new properties, we sought to optimize the transmetallation process to obtain the highest exchange efficiency possible while minimizing the use of RE(III) precursors. As such, the degree of transmetallation in Y-CU-10 with several RE(III) ions was evaluated using 5 equivalents of RE(III) precursor in DMF at 140 ºC for 3, 7 and 14 days (Figure 2a, Table S4). After 14 days, the metal exchange in Y-CU-10 was found to be higher than 70 % when using seven rare-earth metals: La(III), Nd(III), Eu(III), Tb(III), Er(III), Tm(III), and Yb(III). Furthermore, these experiments were completed in quadruplicates and the amount of Y(III) exchanged was found to be highly reproducible. Ultimately, these results indicate that 6 or more of the 9 Y(III) ions in the metal cluster node of Y-CU-10 can be exchanged under these conditions optimized for a balance of cost and efficiency (Figure 2b).

To confirm the structural integrity of the post-synthetically modified RE-CU-10 analogues, PXRD was performed. Upon close inspection of the reflections found in the patterns pre- and post-transmetallation, it can be stated that the bulk of the material remains structurally the same, as no considerable changes in the diffraction patterns were observed (Figure 3). Nonetheless, the crystallinity of the daughter RE-CU-10 analogues varies as a function of RE(III) ion (Figure S5). Since there is no evidence of new crystalline phases being formed, this variation in crystallinity can be attributed to a partial amorphization of the material. Interestingly, the crystallinity of the daughter RE-CU-10 analogues is clearly associated with the ionic radii of the RE(III) used, where an increase in iodic radius – towards the lighter lanthanoids – seems to
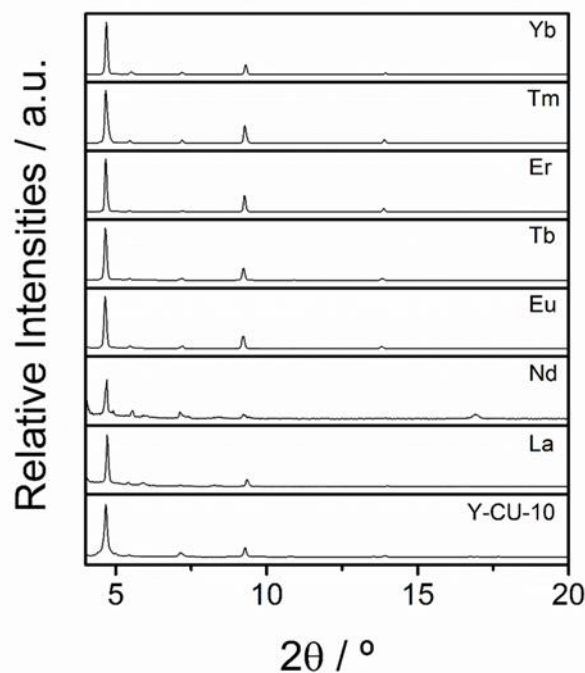

Figure. 4. N$_2$ sorption isotherms of Y-CU-10 and the transmetallated RE-CU-10 analogues.

weaken the structure and lead to a greater decrease in bulk crystallinity of the material. It is well-known that carboxylates of larger RE(III) ions prefer higher coordination numbers (CNs), so when Y(III) (CN = 8) is replaced with lanthanoids from La(III) to Nd(III) (preferred CN = 9) these ions are less likely to adapt to the lower coordination number environment.[54] It is possible that when trying accommodate a CN of 9 in these larger ions, there are steric issues that lead to instability of the nonanuclear cluster, resulting in partial amorphization of the material. This hypothesis is further supported by studying the crystallinity of Y-CU-10 exchanged with La(III). After 3 days reaction, the transmetallation rate follows the same trend as that observed for the other RE metals, where approximately 3 of the 9 Y(III) ions of the cluster are exchanged, and only a small decrease in the bulk crystallinity is observed (Figure 2a, Figure S6). Whereas after 7 days, approximately 6 of the 9 Y(III) ions are exchanged, accounting for a more marked decrease in bulk crystallinity. Finally, after 14 days, approximately 8 of the 9 Y(III) ions in the cluster are exchanged for La(III), a clear deviation (> 10%) in comparison with the heavier lanthanoids, and the crystallinity of the material has greatly decreased. This suggests there is a threshold in the percentage of Y(III) (CN = 8) that can be exchanged with larger lanthanoids (preferred CN = 9) in the nonanuclear cluster before the system collapses.

To evaluate the effects of transmetallation on the surface area of CU-10, nitrogen sorption isotherms were collected and used to calculate BET surface areas. As can be seen in Figure 4, all materials display the expected reversible Type-I(a) isotherm.[55] While the parent MOF, Y-CU-10, displays a BET surface area of 1790 m^2 g^{-1}, a slight decrease in surface area is observed for the heavier lanthanoids: Eu (1400 m^2 g^{-1}), Tb (1470 m^2 g^{-1}), Er (1720 m^2 g^{-1}), Tm (1520 m^2 g^{-1}), and Yb (1360 m^2 g^{-1}). The surface areas of these

Figure. 3. Normalized PXRD patterns of Y-CU-10, as well as the MOF after metal exchange with La(III), Nd(III), Eu(III), Tb(III), Er(III), Tm(III), and Yb(III).
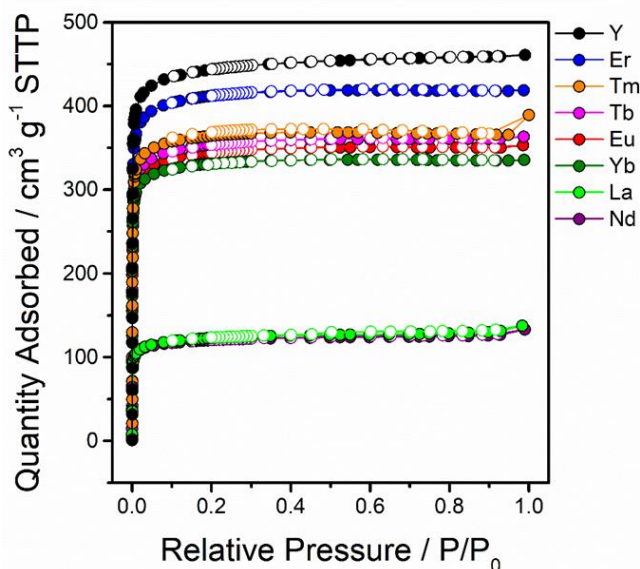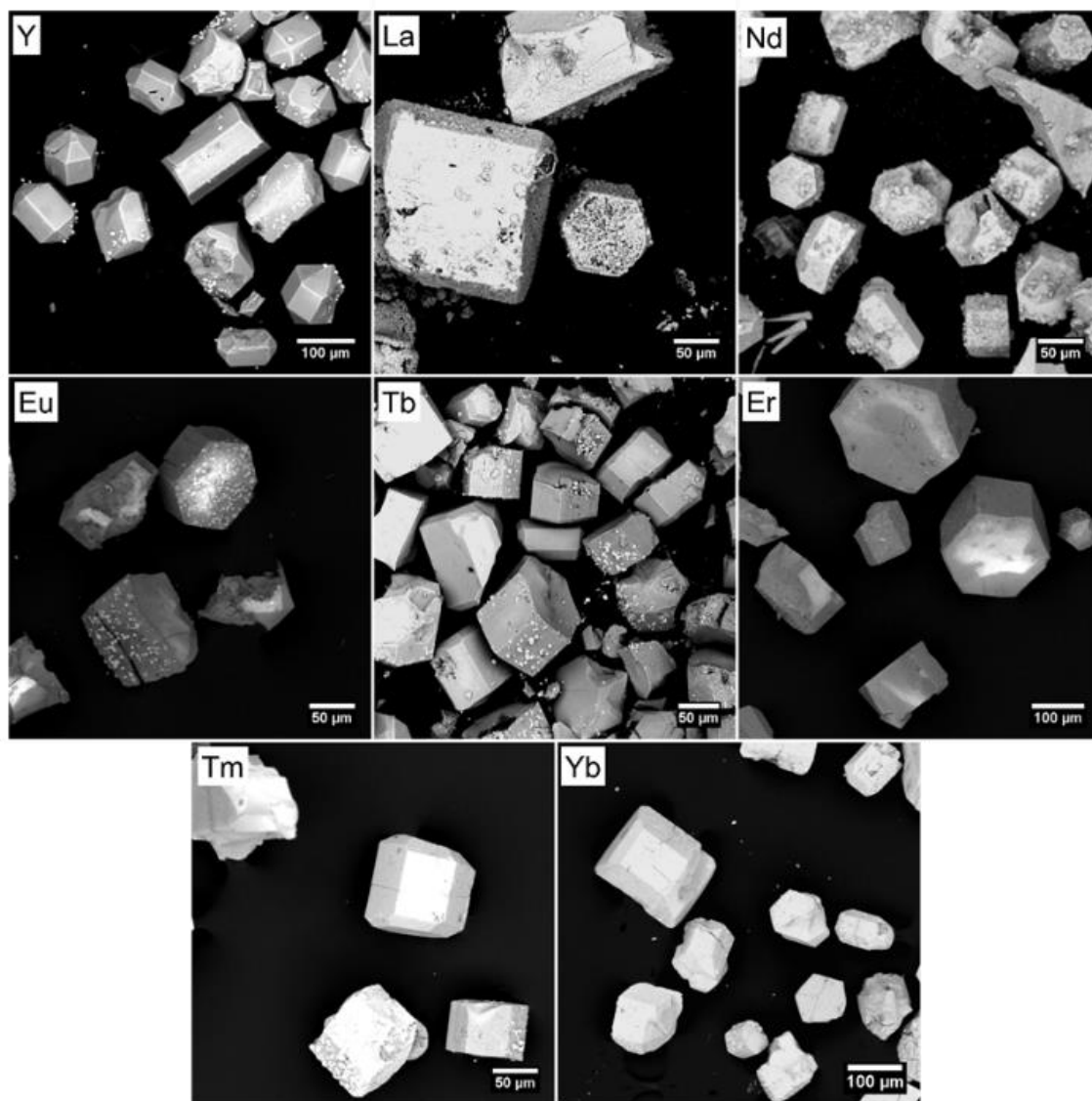
Figure. 5. SEM micrographs of the parent Y-CU-10 and the metal-exchanged MOFs.

daughter RE-CU-10 analogues are decreased compared to the parent MOF due to the presence of heavier RE(III) ions, the use of activation procedures that were optimized for Y-CU-10 only, and in the case of Eu(III) and Tb(III) a small degree of amorphization of the material. On the other hand, the early lanthanoids, La and Nd, demonstrated a steep drop in surface area: La (480 m^2 g^{-1}) and Nd (475 m^2 g^{-1}), consistent with the observed decrease in crystallinity and partial amorphization of these CU-10 analogues.

In order to obtain a more complete understanding of the location of the new RE(III) ions exchanged in Y-CU-10, SEM micrographs coupled with EDS data were obtained. As shown in Figure 5, crystals with hexagonal prismatic shapes consistent with the **shp** topology are observed for Y-CU-10 and for all transmetallated MOFs. However, the Y-CU-10 analogues exchanged with early lanthanoids (i.e., La(III), and Nd(III)) clearly show a rough surface, possibly indicating the formation of structural defects. Consistent with PXRD and nitrogen sorption data, the surface roughness of these materials increases with increasing ionic radii of the

incoming RE(III) ion. On the other hand, the transmetallated samples containing Er(III), Tm(III), and Yb(III) have well-defined hexagonal morphology, nearly identical to the parent Y-CU-10. Additionally, EDS line scan analysis was performed on single crystallites of all transmetallated samples (Figures S7-S13). In all cases, homogeneous distributions of the lanthanoids and Y could be observed, indicating that the metal-exchange process is indeed taking place throughout the framework, rather than on the external surface only.

Finally, to unequivocally confirm that RE(III) ions are being introduced into the nonanuclear cluster of Y-CU-10, single crystal X-ray diffraction was performed on a single crystal of the transmetallated Tm(III) analogue (Table S5). Our group, and others have shown that the nonanuclear cluster node in Y-CU-10, Tb-CU-10 and other RE(III)-**shp**-MOFs is disordered over two positions.[45,56] SCXRD performed on the transmetallated Tm(III) analogue shows that, in both nonanuclear clusters, 6 of the 9 Y(III) ions are replaced with Tm(III). When analyzing the double six membered ring (d6r) building unit of CU-10 (Figure 6), the top and bottom

rings are comprised of Tm(III) ions, while the middle layer is comprised of Y(III). This result is consistent with the ~70 % exchange determined using ICP-MS.
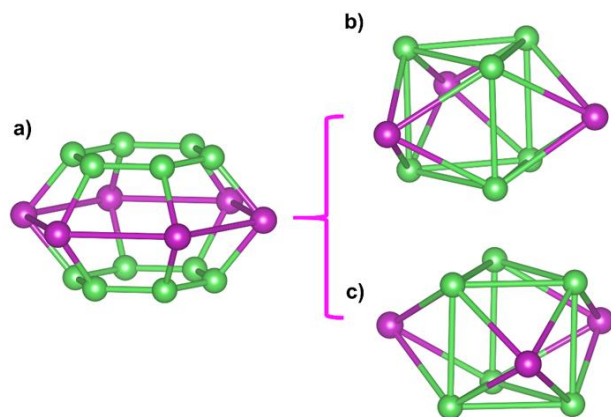

Figure. 6. Representation of (a) the transmetallated disordered RE$_9$ cluster (appearing as a RE$_{18}$ cluster), and separated into nonanuclear building units: (b) and (c).

4. Conclusions

In summary, post-synthetic modification of Y-CU-10 was performed by transmetallation of Y(III) using seven different RE ions: La(III), Nd(III), Eu(III), Tb(III), Er(III), Tm(III), and Yb(III). By optimizing the reaction conditions for cost and efficiency, all seven daughter MOFs displayed transmetallation rates higher than 70 %. Characterization of the daughter materials indicates that the overall network structure of CU-10 is maintained after the transmetallation process. However, the metal-exchanged La- and Nd-CU-10 analogues clearly demonstrate a higher degree of amorphization of the structure, which can be attributed to their higher ionic radii and different coordination number preferences, compared to the other RE(III) ions. Finally, SCXRD measurements on transmetallated Tm-CU-10 confirmed that the Y(III) ions were replaced by Tm(III) in the nonanuclear clusters of the MOF with a ratio of Y:Tm of 3:6, matching the results obtained by ICP-MS. These results shine light on the use of transmetallation in RE cluster-based MOFs, something that has not been explored in the literature before. The example here shows that by simply adjusting the reaction parameters, partial or near-complete transmetallation can be accomplished, with the potential to give new RE-MOF analogues with unique properties and applications.

ASSOCIATED CONTENT

All transmetallation data, SEM-EDS micrographs, raw ICP-MS data and calculations, and single-crystal X-ray diffraction data are provided. The crystal structure of Tm-CU-10 was deposited in the Cambridge Crystallographic Data Centre (CCDC), deposition number 2079223.

AUTHOR INFORMATION

Corresponding Author

*ashlee.howarth@concordia.ca
Tel. +1 (514) 848-2424 ext. 5324

Author Contributions

All authors have given approval to the final version of the manuscript.

Notes

The authors declare no competing financial interest.

REFERENCES

(1)   Batten, S. R.; Champness, N. R.; Chen, X. M.; Garcia-Martinez, J.; Kitagawa, S.; Öhrström, L.; O'Keeffe, M.; Suh, M. P.; Reedijk, J. Terminology of Metal-Organic Frameworks and Coordination Polymers (IUPAC Recommendations 2013). *Pure Appl. Chem.* **2013**, *85* (8), 1715–1724.

(2)   Batten, S. R.; Champness, N. R.; Chen, X. M.; Garcia-Martinez, J.; Kitagawa, S.; Öhrström, L.; O'Keeffe, M.; Suh, M. P.; Reedijk, J. Coordination Polymers, Metal-Organic Frameworks and the Need for Terminology Guidelines. *CrystEngComm* **2012**, *14* (9), 3001–3004.

(3)   Kondo, M.; Yoshitomi, T.; Seki, K.; Matsuzaka, H.; Kitagawa, S. Three-Dimensional Framework with Channeling Cavities for Small Molecules: {[M2(4,4'-Bpy)₃(NO3)₄].XH₂O}n (M = Co, Ni, Zn). *Angew. Chemie* **1997**, *36* (16), 1725–1727.

(4)   Cheetham, A. K.; Férey, G.; Loiseau, T. Open-Framework Inorganic Materials. *Angew. Chemie* **1999**, *38*, 3268–3292.

(5)   Hoskins, B. F.; Robson, R. Design and Construction of a New Class of Scaffolding-like Materials Comprising Infinite Polymeric Frameworks of 3D-Linked Molecular Rods. A Reappraisal of the Zn(CN)2 and Cd(CN)2 Structures and the Synthesis and Structure of the Diamond-Related Framework. *J. Am. Chem. Soc.* **1990**, *112* (4), 1546–1554.

(6)   Yaghi, O. M.; Li, H. Hydrothermal Synthesis of a Metal-Organic Framework Containing Large Rectangular Channels. *J. Am. Chem. Soc.* **1995**, *117* (41), 10401–10402.

(7)   Moosavi, S. M.; Nandy, A.; Jablonka, K. M.; Ongari, D.; Janet, J. P.; Boyd, P. G.; Lee, Y.; Smit, B.; Kulik, H. J. Understanding the Diversity of the Metal-Organic Framework Ecosystem. *Nat. Commun.* **2020**, *11* (1), 4068.

(8)   Lee, J.; Farha, O. K.; Roberts, J.; Scheidt, K. A.; Nguyen, S. T.; Hupp, J. T. Metal-Organic Framework Materials as Catalysts. *Chem. Soc. Rev.* **2009**, *38* (5), 1450–1459.

(9)   Otake, K. I.; Cui, Y.; Buru, C. T.; Li, Z.; Hupp, J. T.; Farha, O. K. Single-Atom-Based Vanadium Oxide Catalysts Supported on Metal-Organic Frameworks: Selective Alcohol Oxidation and

Structure-Activity Relationship. *J. Am. Chem. Soc.* **2018**, *140* (28), 8652–8656.

(10) Wang, C.; An, B.; Lin, W. Metal-Organic Frameworks in Solid-Gas Phase Catalysis. *ACS Catal.* **2019**, *9* (1), 130–146.

(11) Yang, D.; Gates, B. C. Catalysis by Metal Organic Frameworks: Perspective and Suggestions for Future Research. *ACS Catal.* **2019**, *9* (3), 1779–1798.

(12) Xue, D. X.; Belmabkhout, Y.; Shekhah, O.; Jiang, H.; Adil, K.; Cairns, A. J.; Eddaoudi, M. Tunable Rare Earth Fcu-MOF Platform: Access to Adsorption Kinetics Driven Gas/Vapor Separations via Pore Size Contraction. *J. Am. Chem. Soc.* **2015**, *137* (15), 5034–5040.

(13) Mason, J. A.; Veenstra, M.; Long, J. R. Evaluating Metal-Organic Frameworks for Natural Gas Storage. *Chem. Sci.* **2014**, *5* (1), 32–51.

(14) Ma, S.; Zhou, H. C. A Metal-Organic Framework with Entatic Metal Centers Exhibiting High Gas Adsorption Affinity. *J. Am. Chem. Soc.* **2006**, *128* (36), 11734–11735.

(15) Kreno, L. E.; Leong, K.; Farha, O. K.; Allendorf, M.; Van Duyne, R. P.; Hupp, J. T. Metal-Organic Framework Materials as Chemical Sensors. *Chem. Rev.* **2012**, *112* (2), 1105–1125.

(16) Bauer, C. A.; Timofeeva, T. V.; Settersten, T. B.; Patterson, B. D.; Liu, V. H.; Simmons, B. A.; Allendorf, M. D. Influence of Connectivity and Porosity on Ligand-Based Luminescence in Zinc Metal-Organic Frameworks. *J. Am. Chem. Soc.* **2007**, *129* (22), 7136–7144.

(17) Zhang, X.; Ballem, M. A.; Hu, Z. J.; Bergman, P.; Uvdal, K. Nanoscale Light-Harvesting Metal-Organic Frameworks. *Angew. Chemie - Int. Ed.* **2011**, *50* (25), 5729–5733.

(18) Yaghi, O. M.; O'Keeffe, M.; Ockwig, N. W.; Chae, H. K.; Eddaoudi, M.; Kim, J. Reticular Synthesis and the Design of New Materials. *Nature* **2003**, *423* (6941), 705–714.

(19) Goesten, M. G.; Kapteijn, F.; Gascon, J. Fascinating Chemistry or Frustrating Unpredictability: Observations in Crystal Engineering of Metal-Organic Frameworks. *CrystEngComm* **2013**, *15* (45), 9249–9257.

(20) Tanabe, K. K.; Cohen, S. M. Postsynthetic Modification of Metal–Organic Frameworks—a Progress Report. *Chem. Soc. Rev.* **2011**, *40* (2), 498–519.

(21) Deria, P.; Mondloch, J. E.; Karagiaridi, O.; Bury, W.; Hupp, J. T.; Farha, O. K. Beyond Post-Synthesis Modification: Evolution of Metal-Organic Frameworks via Building Block Replacement. *Chem. Soc. Rev.* **2014**, *43* (16), 5896–5912.

(22) Kalaj, M.; Cohen, S. M. Postsynthetic Modification: An Enabling Technology for the Advancement of Metal-Organic Frameworks. *ACS Cent. Sci.* **2020**, *6* (7), 1046–1057.

(23) Grancha, T.; Ferrando-Soria, J.; Zhou, H. C.; Gascon, J.; Seoane, B.; Pasán, J.; Fabelo, O.; Julve, M.; Pardo, E. Postsynthetic Improvement of the Physical Properties in a Metal-Organic Framework through a Single Crystal to Single Crystal Transmetallation. *Angew. Chemie - Int. Ed.* **2015**, *54* (22), 6521–6525.

(24) Wang, Z.; Cohen, S. M. Postsynthetic Covalent Modification of a Neutral Metal-Organic Framework. *J. Am. Chem. Soc.* **2007**, *129* (41), 12368–12369.

(25) Karagiaridi, O.; Bury, W.; Mondloch, J. E.; Hupp, J. T.; Farha, O. K. Solvent-Assisted Linker Exchange: An Alternative to the de Novo Synthesis of Unattainable Metal-Organic Frameworks. *Angew. Chemie - Int. Ed.* **2014**, *53* (18), 4530–4540.

(26) Kim, M.; Cahill, J. F.; Su, Y.; Prather, K. A.; Cohen, S. M. Postsynthetic Ligand Exchange as a Route to Functionalization of "Inert" Metal-Organic Frameworks. *Chem. Sci.* **2012**, *3* (1), 126–130.

(27) Smith, S. J. D.; Konstas, K.; Lau, C. H.; Gozukara, Y. M.; Easton, C. D.; Mulder, R. J.; Ladewig, B. P.; Hill, M. R. Post-Synthetic Annealing: Linker Self-Exchange in UiO-66 and Its Effect on Polymer-Metal Organic Framework Interaction. *Cryst. Growth Des.* **2017**, *17* (8), 4384–4392.

(28) Dincă, M.; Long, J. R. High-Enthalpy Hydrogen Adsorption in Cation-Exchanged Variants of the Microporous Metal-Organic Framework $Mn_3[(Mn_4Cl)_3(BTT)_8(CH_3OH)_{10}]_2$. *J. Am. Chem. Soc.* **2007**, *129* (36), 11172–11176.

(29) Lalonde, M.; Bury, W.; Karagiaridi, O.; Brown, Z.; Hupp, J. T.; Farha, O. K. Transmetalation: Routes to Metal Exchange within Metal-Organic Frameworks. *J. Mater. Chem. A* **2013**, *1* (18), 5453–5468.

(30) Islamoglu, T.; Goswami, S.; Li, Z.; Howarth, A. J.; Farha, O. K.; Hupp, J. T. Postsynthetic Tuning of Metal-Organic Frameworks for Targeted Applications. *Acc. Chem. Res.* **2017**, *50* (4), 805–813.

(31) Mondloch, J. E.; Bury, W.; Fairen-Jimenez, D.; Kwon, S.; Demarco, E. J.; Weston, M. H.; Sarjeant, A. A.; Nguyen, S. T.; Stair, P. C.; Snurr, R. Q.; Farha, O. K.; Hupp, J. T. Vapor-Phase Metalation by Atomic Layer Deposition in a Metal-Organic Framework. *J. Am. Chem. Soc.* **2013**, *135* (28), 10294–10297.

(32) Liu, T. F.; Vermeulen, N. A.; Howarth, A. J.; Li, P.; Sarjeant, A. A.; Hupp, J. T.; Farha, O. K. Adding to the Arsenal of Zirconium-Based Metal–Organic Frameworks: The Topology as a Platform for Solvent-Assisted Metal Incorporation. *Eur. J. Inorg. Chem.* **2016**, *2016* (27), 4349–4352.

(33) Yuan, S.; Chen, Y. P.; Qin, J.; Lu, W.; Wang, X.; Zhang, Q.; Bosch, M.; Liu, T. F.; Lian, X.; Zhou, H. C. Cooperative Cluster Metalation and Ligand Migration in Zirconium Metal-Organic Frameworks. *Angew. Chemie - Int. Ed.* **2015**, *54* (49), 14696–14700.

(34) Mandal, S.; Natarajan, S.; Mani, P.; Pankajakshan, A. Post-Synthetic Modification of Metal–Organic Frameworks Toward Applications. *Adv. Funct. Mater.* **2021**, *31* (4), 2006291.

(35) Saraci, F.; Quezada-Novoa, V.; Donnarumma, P. R.; Howarth, A. J. Rare-Earth Metal-Organic Frameworks: From Structure to Applications. *Chem. Soc. Rev.* **2020**, *49* (22), 7949–7977.

(36) Pagis, C.; Ferbinteanu, M.; Rothenberg, G.; Tanase, S. Lanthanide-Based Metal Organic Frameworks: Synthetic Strategies and Catalytic Applications. *ACS Catal.* **2016**, *6*, 6063–6072.

(37) Das, S.; Kim, H.; Kim, K. Metathesis in Single Crystal: Complete and Reversible Exchange of Metal Ions Constituting the Frameworks of Metal-Organic Frameworks. *J. Am. Chem. Soc.* **2009**, *131* (11), 3814–3815.

(38) Seth, S.; Savitha, G.; Moorthy, J. N. Diverse Isostructural MOFs by Postsynthetic Metal Node Metathesis: Anionic-to-Cationic Framework Conversion, Luminescence and Separation of Dyes. *J. Mater. Chem. A* **2015**, *3* (45), 22915–22922.

(39) Asha, K. S.; Bhattacharjee, R.; Mandal, S. Complete Transmetalation in a Metal-Organic Framework by Metal Ion Metathesis in a Single Crystal for Selective Sensing of Phosphate Ions in Aqueous Media. *Angew. Chemie* **2016**, *128* (38), 11700–11704.

(40) Ding, W.; Zhao, L.; Yuan, X.; Zhang, L.; Chen, B.; Ju, Q.; Fang, Z. Multicolour Barcoding in One MOF Crystal through Rational Postsynthetic Transmetalation. *J. Mater. Chem. C* **2020**, *8* (9), 3176–3182.

(41) Yang, Y.; Zhao, L.; Sun, M.; Wei, P.; Li, G.; Li, Y. Highly Sensitive Luminescent Detection toward Polytypic Antibiotics by a Water-Stable and White-Light-Emitting MOF-76 Derivative. *Dye. Pigment.* **2020**, *180*, 108444.

(42) Wang, P.; Ma, J. P.; Dong, Y. Bin; Huang, R. Q. Tunable Luminescent Lanthanide Coordination Polymers Based on Reversible Solid-State Ion-Exchange Monitored by Ion-Dependent Photoinduced Emission Spectra. *J. Am. Chem. Soc.* **2007**, *129* (35), 10620–10621.

(43) Lv, X. L.; Feng, L.; Xie, L. H.; He, T.; Wu, W.; Wang, K. Y.; Si, G.; Wang, B.; Li, J. R.; Zhou, H. C. Linker Desymmetrization: Access to a Series of Rare-Earth Tetracarboxylate Frameworks with Eight-Connected Hexanuclear Nodes. *J. Am. Chem. Soc.* **2021**, *143* (7), 2784–2791.

(44) Wang, T. C.; Vermeulen, N. A.; Kim, I. S.; Martinson, A. B. F.; Fraser Stoddart, J.; Hupp, J. T.; Farha, O. K. Scalable Synthesis and Post-Modification of a Mesoporous Metal-Organic Framework Called NU-1000. *Nat. Protoc.* **2016**, *11* (1), 149–162.

(45) Quezada-novoa, V.; Titi, H. M.; Sarjeant, A.; Howarth, A. Building a Shp: A New Rare-Earth Metal-Organic Framework and

Its Application in a Catalytic Photo-Oxidation Reaction. *ChemRxiv* **2020**, *Preprint*.

(46)   Xue, D.-X.; Cairns, A. J.; Belmabkhout, Y.; Wojtas, L.; Liu, Y.; Alkordi, M.; Eddaoudi, M. Tunable Rare-Earth Fcu-MOFs: A Platform for Systematic Enhancement of CO2 Adsorption Energetics and Uptake. *J. Am. Chem. Soc.* **2013**, *135*, 7660–7667.

(47)   Jiang, H.; Jia, J.; Shkurenko, A.; Chen, Z.; Adil, K.; Belmabkhout, Y.; Weselinski, L. J.; Assen, A. H.; Xue, D.-X.; O'Keefe, M.; Eddaoudi, M. Enriching the Reticular Chemistry Repertoire: Merged Nets Approach for the Rational Design of Intricate Mixed-Linker Metal–Organic Framework Platforms. *J. Am. Chem. Soc.* **2018**, *140*, 8858–8867.

(48)   Zhang, L.; Yuan, S.; Feng, L.; Guo, B.; Qin, J.; Xu, B.; Lollar, C.; Sun, D.; Zhou, H. Pore-Environment Engineering with Multiple Metal Sites in Rare- Earth Porphyrinic Metal–Organic Frameworks. *Angew. Chemie - Int. Ed.* **2018**, *57*, 5095–5099.

(49)   Wang, Y.; Feng, L.; Fan, W.; Wang, K.-Y.; Wang, X.; Wang, X.; Zhang, K.; Zhang, X.; Dai, F.; Sun, D.; Zhou, H.-C. Topology Exploration in Highly Connected Rare-Earth Metal–Organic Frameworks via Continuous Hindrance Control. *J. Am. Chem. Soc.* **2019**, *141*, 6967–6975.

(50)   Prasad, T. K.; Hong, D. H.; Suh, M. P. High Gas Sorption and Metal-Ion Exchange of Microporous Metal–Organic Frameworks with Incorporated Imide Groups. *Chem. - A Eur. J.* **2010**, *16*, 14043–14050.

(51)   Song, X.; Jeong, S.; Kim, D.; Lah, M. S. Transmetalations in Two Metal–Organic Frameworks with Different Framework Flexibilities: Kinetics and Core–Shell Heterostructure. *Cryst. Growth Des.* **2012**, *14*, 5753–5756.

(52)   Pal, T. K.; De, D.; Senthilkumar, S.; Neogi, S.; Bharadwaj, P. K. A Partially Fluorinated, Water-Stable Cu(II)–MOF Derived via Transmetalation: Significant Gas Adsorption with High CO2 Selectivity and Catalysis of Biginelli Reactions. *Inorg. Chem.* **2016**, *55*, 7835–7842.

(53)   Balestri, D.; Bassanetti, I.; Canossa, S.; Gazzurelli, C.; Bacchi, A.; Bracco, S.; Comotti, A.; Pelagatti, P. Changing the Dress to a MOF through Fluorination and Transmetalation. Structural and Gas-Sorption Effects. *Cryst. Growth Des.* **2018**, *18*, 6824–6832.

(54)   Janicki, R.; Mondry, A.; Starynowicz, P. Carboxylates of Rare Earth Elements. *Coord. Chem. Rev.* **2017**, *340*, 98–133.

(55)   Thommes, M.; Kaneko, K.; Neimark, A. V.; Olivier, J. P.; Rodriguez-Reinoso, F.; Rouquerol, J.; Sing, K. S. W. Physisorption of Gases, with Special Reference to the Evaluation of Surface Area and Pore Size Distribution (IUPAC Technical Report). *Pure Appl. Chem.* **2015**, *87* (9–10), 1051–1069.

(56)   Chen, Z.; Weselinski, L. J.; Adil, K.; Belmabkhout, Y.; Shkurenko, A.; Jiang, H.; Bhatt, P. M.; Guillerm, V.; Dauzon, E.; Xue, D.-X.; O'Keeffe, M.; Eddaoudi, M. Applying the Power of Reticular Chemistry to Finding the Missing Alb-MOF Platform Based on the (6,12)-Coordinated Edge-Transitive Net. *J. Am. Chem. Soc.* **2017**, *139*, 3265–3274.

SYNOPSIS TOC (Word Style "SN_Synopsis_TOC"). If you are submitting your paper to a journal that requires a synopsis graphic and/or synopsis paragraph, see the Instructions for Authors on the journal's homepage for a description of what needs to be provided and for the size requirements of the artwork.

Insert Table of Contents artwork here